CHEMISTRY OF MATERIALS

Article

pubs.acs.org/cm

Aqueous Molecular Sieving and Strong Gas Adsorption in Highly Porous MOFs with a Facile Synthesis

Mainak Majumder,[†] Phillip Sheath,[†] James I. Mardel,[‡] Timothy G. Harvey,[‡] Aaron W. Thornton,[‡] Amanda Gonzago,[†] Danielle F. Kennedy,[‡] Ian Madsen,[§] James W. Taylor,[†] David R. Turner,[∥] and Matthew R. Hill*[,‡]

[†]Nanoscale Science and Engineering Laboratories (NSEL), Department of Mechanical Engineering, Monash University, Clayton VIC Australia 3168

[‡]CSIRO Materials Science and Engineering, Private Bag 33, Clayton South MDC VIC 3169, Australia

[§]CSIRO Process Science and Engineering, Private Bag 33, Clayton South MDC VIC 3169, Australia

[∥]School of Chemistry, Monash University, Clayton VIC Australia 3168

Supporting Information

ABSTRACT: Aqueous molecular sieving is demonstrated in a new series of isostructural metal organic frameworks based on the perylene tetracarboxylate (PTC) ligand. The frameworks can be formed in water at room temperature with Mg, Ni, and other first row transition metal ions and adopt a highly porous topology that results in predicted surface areas of over 2000 $m^2\ g^{-1}$ and periodic channels of around 6 Å in diameter. Unusually, the M-PTC MOFs are highly resistant to moisture and can be readily synthesized on multigram scales. The frameworks have been shown to exhibit molecular sieving in the absorption from mixtures of organic molecules at low aqueous concentrations, with an application demonstrated on a dangerous water-borne herbicide, Paraquat. Ni-PTC also exhibits a structural flexibility that leads to strong and selective gas adsorption characteristics, with an IAST selectivity of 300 for carbon dioxide being adsorbed over nitrogen. Binding enthalpies for hydrogen and carbon dioxide are also very strong in comparison to other MOFs, at 10.75 and 52.50 kJ/mol respectively.

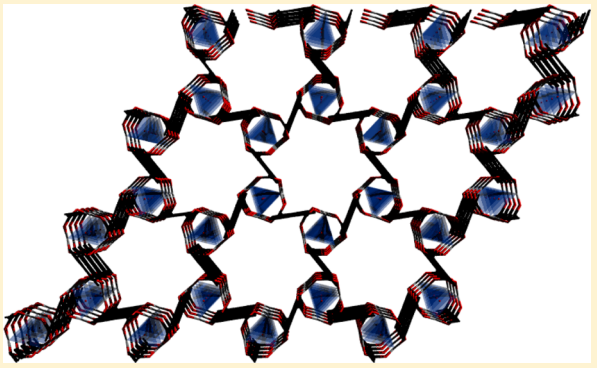

KEYWORDS: *metal organic framework, MOF, carbon dioxide capture, hydrogen storage, molecular sieving, capture of toxins*

Metal organic frameworks (MOFs) are potentially paradigm shifting materials due to their ultrahigh porosity, for which both the pore size and pore surface chemistry is tunable.[1] Consisting of metal atoms or clusters joined periodically to one another by organic ligands, the uniform pores can be used to store,[2−6] separate,[7−10] capture,[11,12] or release[13] materials of interest.

One area in which MOFs are highly suited yet largely untested is molecular sieving in aqueous environments, where it is the uniform pore sizes of MOFs that are most attractive. Other porous capture materials such as carbons,[14,15] silicas,[16−19] or mesoporous metal oxides[20−22] possess pores in the right size range, but their distribution is wide enough so as to limit selectivity. Zeolites have periodic porosity, but the pores are often too small to admit infiltration of organic molecules. In both cases, nonselective absorption to an external surface is a further inherent limitation. MOFs have periodic pores in the right size range to absorb organic molecules and negligible external surface areas. They have been previously employed in the separation of large dye molecules, both through absorption and chromatographic means.[23−25] In the field of environmental toxins, this inherent selectivity can be crucial, as potential toxins are most commonly present in low concentrations, albeit at levels that may still be harmful. High selectivities are likely required to avoid saturation of the pores by nontarget species. Example target systems include dioxins, soluble aromatics, and pesticides, all often found in aqueous media at low but dangerous concentrations.

The use of MOFs for the separation and storage of gases has risen to prominence in recent years. This is due not only to the potential to store vehicular fuels[26] or carbon dioxide in large quantities[27,28] but also to the versatility in the pore surface chemistry which can promote selective capture of one gas over another when the adsorption interaction is sufficiently strong.[29] Selectivity can be controlled by factors such as pore size,[30] exposed metal sites,[31] and ligand chemistry.[32]

Most MOFs do not lend themselves to the capture of environmental toxins due to their instability to water, both as a

Received: June 4, 2012
Revised: November 26, 2012
Published: December 2, 2012

ACS Publications © 2012 American Chemical Society

dx.doi.org/10.1021/cm301726k | *Chem. Mater.* 2012, 24, 4647−4652

liquid or a vapor.[33] Typically, this is due to the metal clusters being prone to hydroxylation, causing a breaking of the metal-to-ligand bonds. Recently, some MOF families have been discovered that exhibit stability in water, where the metal-to-ligand bond is strengthened,[34,35] and hence the propensity to hydrolyze is reduced. Successful approaches include bonding first row transition metals coordinated to linkers via sp^2 hybridized N-donor groups with high pK_a,[36−38] highly interconnected structures,[39] or use of metal carboxylate chemistry where the coordination is particularly strong, such as Zr,[39] Ti,[40] or members of the lanthanide series.[41] However, the formation of some of these materials requires highly energetic synthesis conditions and/or harsh solvents. These conditions are required in order to develop an equilibrium in the reaction mixture that delivers extended structures free of mis-formed bonds, something that is harder to achieve in systems where the metal-to-ligand bond is particularly strong.[34,35]

Herein we describe the synthesis of an isomorphous series of MOFs in water at room temperature, to deliver materials that are stable to application in the sequestration of environmental toxins in aqueous systems. The frameworks, $[M_3(\mu_3\text{-}O)(H_2O)_3(PTC)_{1.5}]_n$ which are formed from the potassium salt of perylene-3,4,9,10-tetracarboxylate (K_4PTC) and a metal acetate salt, are isomorphous for Mg, Ni, Co, and Mn and are denoted herein as **M-PTC** (see Figure 1). Single crystal structures have been obtained for the Mg and Ni derivatives, which reveal a remarkable porous topology. We show by complementary experimental and simulation methods that these materials are capable of size selective adsorption of potential environmental toxins and that the relative sensitivity can also be controlled by internal bonding to the pore walls, causing structural changes.

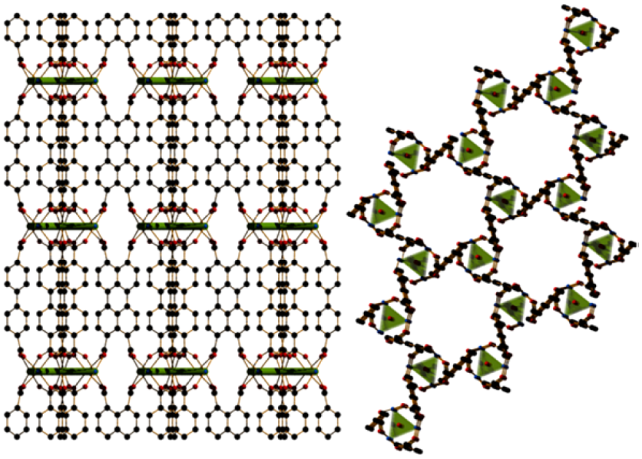

Figure 1. Isotructural M-PTC MOFs $[M_3(\mu_3\text{-}O)(PTC)_{1.5}]_n$ (shown in their fully desolvated state) synthesized in water at room temperature, useful for selective sequestration on environmental toxins. View down the *b*-axis (left), *c*-axis (right). M_3O clusters are highlighted in green.

EXPERIMENTAL DETAILS

Synthesis of K_4PTC. This material was prepared by an adaptation to a literature method.[42] Perylene *p*-dianhydride (20.0 g, 0.051 mol) was added to a 2 M aqueous solution containing 4.2 equivalents of KOH. The resulting red suspension was refluxed overnight to deliver a luminecsent yellow solution. This solution was added dropwise to 2 L of acetone, and a yellow precipitate was formed immediately. The resulting powder was collected and washed with several aliquots of water without being allowed to become dry (drying of the powder while KOH residues remained resulted in dehydration of the salt and a reformation of the anhydride starting material) and acetone (3 × 50 mL) and air-dried to deliver the bright yellow powder **K_4PTC** in quantitative yield (see Scheme 1).

Scheme 1. Synthetic Protocol for M-PTC Framework Syntheses

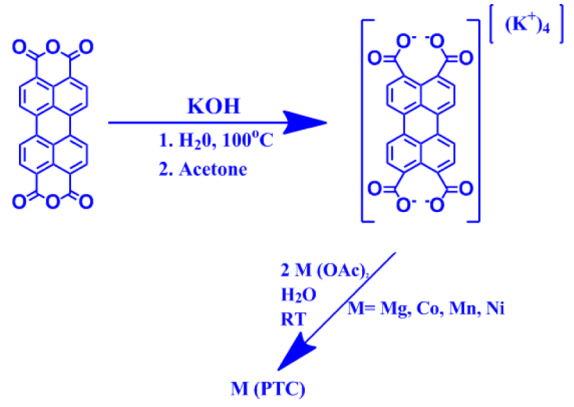

Synthesis of M-PTC Frameworks. 2 mM aqueous solutions of $M(OAc)_2$ (M = Mg, Ni, Co, Mn) (500 mL) and K_4PTC (250 mL) were mixed at room temperature and allowed to stand. After 24 h a crystalline powder consisting of hexagonal orange rods was collected, washed with water, and dried, delivering **M-PTC** in near quantitative yields. XRD traces are included in the Supporting Information.

Characterization Techniques. For dye absorption experiments 10 mg of **Ni-PTC** was weakly ultrasonicated in about 15 mL water for approximately 30 s and placed into an aqueous dye solution (100 mL, ~1.2×10^{-6} M dye concentration). The dye mixture was constantly stirred by magnetic stirring in the dark with aliquots removed at regular intervals to observe the changes of the dye absorbance peak using an Ocean Optics USB-ISS-UV/vis spectrometer. The dyes used were methylene blue, erioglaucine, and methyl viologen from Sigma-Aldrich and Rhodamine B from Exciton.

Single crystal X-ray crystallography was performed on the microcrystallography (MX2) beamline of the Australian Synchrotron at a wavelength of 0.71019 Å using the Blu-Ice[43] interface for data collection and the XDS[44] software package for initial processing (full refinement details in the Supporting Information).

Structure dynamics were explored by subjecting the structure to a series of Molecular Dynamics (MD) simulations with the following details: NPT ensemble, time steps of 0.01 fs, temperature of 298 K using the Nose thermostat and zero pressure using the Andersen Barostat. The aim of these simulations was to discover the different configurations that the structure was capable of forming under various conditions. The Accelrys Materials Studio package was used to implement the MD.

Temperature programmed powder X-ray diffraction was carried out using an Inel diffractometer incorporating the CPS120 position sensitive detector capable of collecting 120° simultaneously. The diffractometer was fitted with a Cu target in a long fine focus tube operated at 40 kV and 40 mA. The samples were housed in a capillary reaction vessel described previously.[45] The sealed end of the capillary was removed and glass wool was used to contain the sample, creating a flow through reactor. The reactor was heated by a stream of hot air, controlling the temperature using a Type-K (chromel/alumel) thermocouple in the center of the air stream and a Eurotherm model 2408 temperature controller. Samples were heated under a constant flow of dry nitrogen at a rate of 5 °C/min, and samples were held at 250 °C for 50 min prior to cooling to ambient temperature. Data collection times of 60 s were used with nominal acquisition time of 65 s. Data were collected continuously throughout the temperature

dx.doi.org/10.1021/cm301726k | Chem. Mater. 2012, 24, 4647−4652

program. Gas adsorption isotherms for pressures in the range of 0−1.2 bar were measured by a volumetric method using a Micromeritics ASAP 2420 instrument. Samples were evacuated and activated at 150 °C under dynamic vacuum at 10^{-6} Torr for 24 h. Accurate sample masses were calculated using degassed samples. Gas adsorption measurements were performed using ultrahigh purity N_2, He, H_2, CO_2, and CH_4 gases.

RESULTS AND DISCUSSION

The **M-PTC** MOFs $[M_3(\mu_3\text{-}O)(H_2O)_3(PTC)_{1.5}]_n$ readily form as a crystalline phase during reaction in water at room temperature. Reaction of two equivalents of metal acetate with K_4PTC led to isolable single crystals for magnesium and nickel derivatives and crystalline powders with manganese and cobalt. Interestingly, amorphous materials were obtained if either the acetate or potassium salts were varied, indicating the fine balance in the reaction kinetics to give crystalline materials under such facile conditions. The reaction conditions have strong implications for large scale usage of these frameworks, given the low energy and environmentally friendly preparation conditions. Indeed the reaction has been found to be scalable, with multiple gram quantities of material able to be generated in a single flask under these conditions. Furthermore, the materials are extremely stable to moisture, with single crystal data able to be collected on dried materials after several months of exposure to the atmosphere. This rare phenomenon among carboxylate MOFs is most likely due to the highly interconnected nature of the material, with each ligand connecting to 4 M_3O structural building units (SBUs).

The **M-PTC** frameworks are isomorphous for the Mg, Co, Ni, and Mn analogues and adopt a highly porous, interconnected topology (see Figure 1). The framework crystallizes in the hexagonal space group $P_{6/m}$ as hydrated materials $[M_3(\mu_3\text{-}O)(H_2O)_3(PTC)_{1.5}]\cdot xH_2O$. The relatively uncommon M_3O structural building unit (SBU) is planar, around a trigonal O^{2-} ligand, with the coordinated aqua ligands being coplanar and six PTC ligands being connected to each SBU (three each above and below the plane bridging between two metals by one carboxylate group). Each metal is octahedrally coordinated, including to one water of solvation, providing a potentially exposed Mg or Ni site upon desolvation. The frameworks contain porous channels of approximately possess an atom-to-atom pore aperture of 1.06 nm, equating to an accessible void space of 0.84 nm. The pores possess unusual surface chemistry, alternating between the hydrophobic perylene units and the hydrophilic metal centers. From single-crystal X-ray data these channels appear to be filled with partially ordered water after synthesis (see the Supporting Information). Calculations using Materials Studio[46] revealed that the Mg and Ni frameworks are highly porous, possessing theoretical BET surface areas of 2008 and 1756 $m^2\ g^{-1}$ respectively. Given the resistance to moisture, unusual hydrophobic channels interspersed by exposed metal sites, and the ready scalability of the synthesis, a myriad of applications are possible with this new family of frameworks. **Mg-PTC** is one of the highest surface area magnesium frameworks reported to date,[3] which is of particular interest for high capacity carbon dioxide and high enthalpy hydrogen storage.[3,47,48]

Based on its promising porosity and stability, **Ni-PTC** was tested for molecular sieving in aqueous environments. As shown in Figure 2, both methylene blue (hydrodynamic radius, HR, 0.49 nm) and the harmful herbicide methyl viologen,

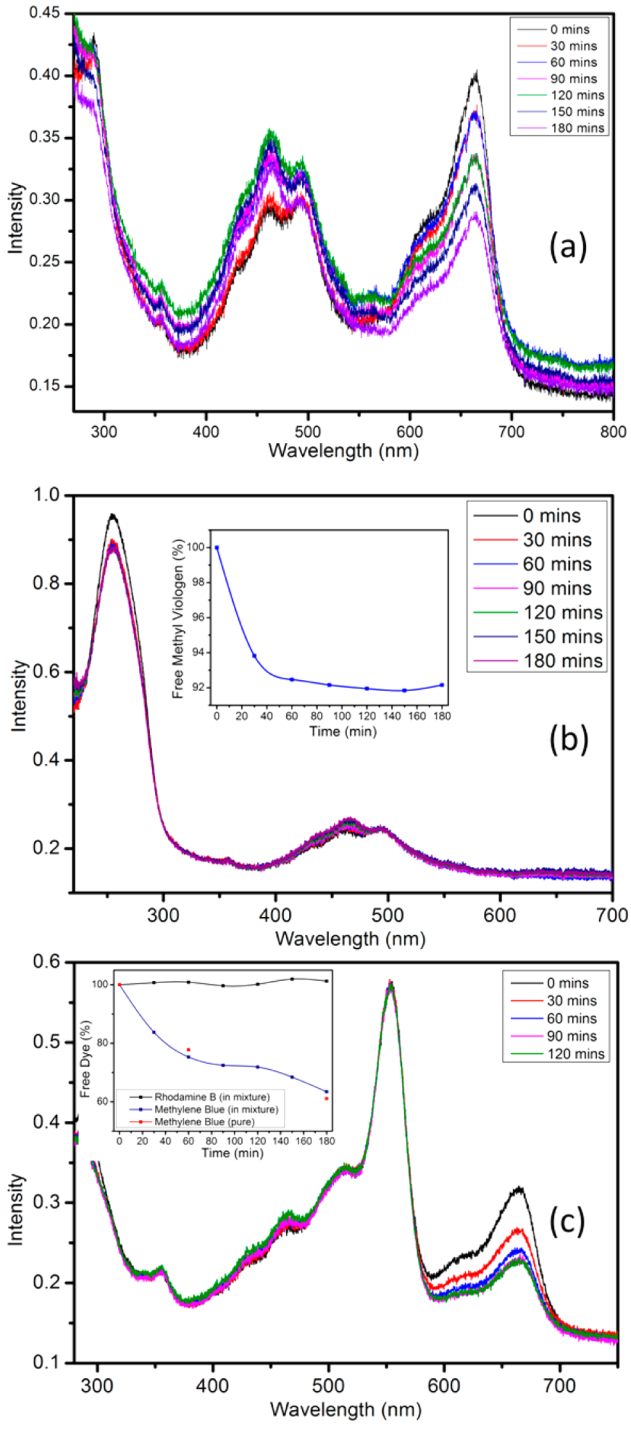

Figure 2. Size-selective adsorption of dyes within **Ni-PTC**. Methylene blue is absorbed in **Ni-PTC** (a), as is methyl viologen (b). Size selectivity was observed, with adsorption rates of methylene blue unchanged in the presence of larger Rhodamine B (c), which does not absorb (c, inset).

Paraquat[49] (HR 0.43 nm), are absorbed from 10^{-6} M aqueous solutions into the framework pores. Absorption of methyl viologen reaches saturation more quickly than for methylene blue (Figure 2b, 2c, inset). Notably absorption characteristics were unchanged when dye mixtures were used, with the larger Rhodamine B (HR 0.65 nm) excluded, while methylene blue was absorbed at the same speed as for a pure mixture (Figure 2c, inset). Further investigation of these aqueous absorption

dx.doi.org/10.1021/cm301726k | Chem. Mater. 2012, 24, 4647−4652

profiles revealed an essentially infinite size selectivity based on the hydrodynamic radii of the dye substrates (Figure 3, bottom).

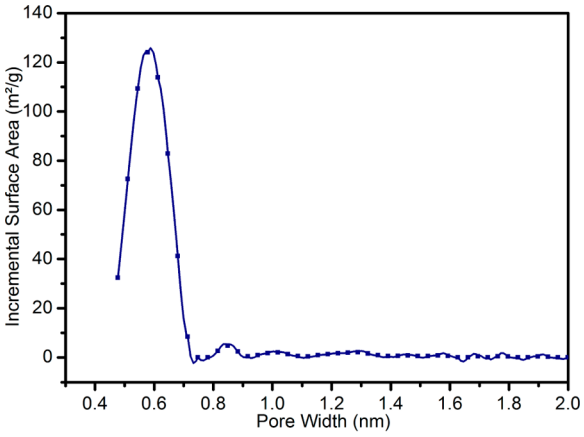

Probe	Peak Wave-length (nm)	Hydrodynamic Radius (nm)	Adsorption in Ni-PTC?
Methyl Viologen	255	0.43	Yes
Methylene Blue	664	0.49	Yes
Rhodamine B	565	0.65	No
Erioglaucine	628	0.78	No

Figure 3. Pore size distribution for **Ni-PTC** calculated with DFT from gas adsorption isotherms (top), which correlates well with the hydrodynamic radii of absorbed dyes (bottom).

Exclusion of larger dyes correlated extremely well with the measured pore size, from DFT fits to gas adsorption isotherms (Figure 3, top) where a uniform pore size of 6 Å was observed. Dyes larger than this were found to be excluded (Figure 3, bottom, also the Supporting Information). The complete absence of absorption of larger dyes is of particular interest given the change in hydrodynamic radii was just 1.6 Å, assigned to the uniform pore size distribution (Figure 3). The result was reconfirmed in experiments involving the larger Erioglaucine, which was not adsorbed (see the Supporting Information SI-11, SI-12). Most MOFs are not available for this application due to their lack of resistance to moisture.[33]

The measured BET surface area of 223 $m^2\ g^{-1}$ is well below the predicted value of 1756 $m^2\ g^{-1}$. Ni-PTC exhibits structural flexibility, but this alone may not be sufficient to account for the large discrepancy in surface area. Temperature dependent XRD of **Ni-PTC** exhibits small structural changes in the material upon desolvation, such as the broadening of the peak at 2° 2θ, diminishment at 7.8^o, and the disappearance of the peak at 11°. Second, energy minimization calculations (Figure 4) show that the observed crystallographic phase is not the most energetically favored when the hydration level is varied, or an absorbent is present. Finally, there is a variation between the calculated, solvated pore size (0.84 nm) with the measured, desolvated pore size (0.60 nm, Figure 3). This alone may not be sufficient to account for this broad discrepancy (Figure 5). Recently Ma et al.[50] reported a breathing effect in MOFs with large pores and were able to exhibit a loss of diffraction peaks upon desolvation, which were regained following resolvation. The

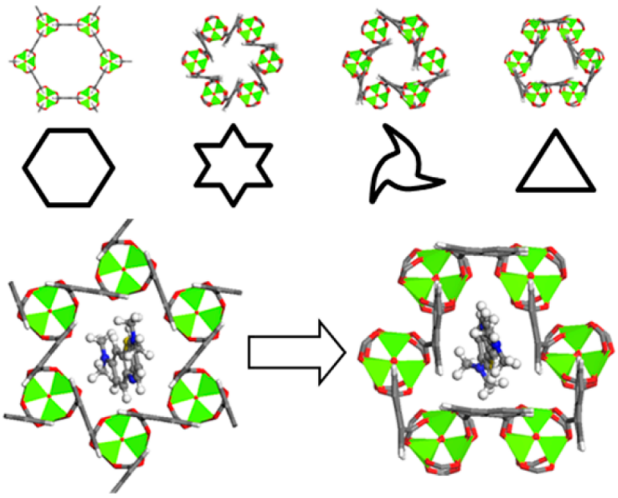

Figure 4. Energy minimization calculations show that the M_3O SBU can readily rotate to give structures with shaped channel apertures (top). In the presence of methylene blue, such rearrangements deliver particularly strong bonding modes (bottom).

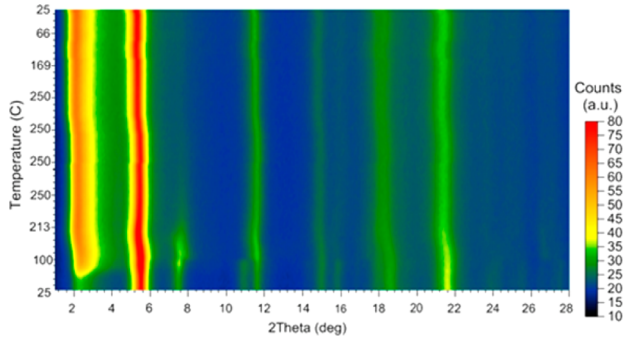

Figure 5. Structural variations are seen with temperature dependent X-ray powder diffraction, in particular as water of solvation is removed.

large, energetically unfavored channels found in this case may also be prone to such a collapse upon evacuation, even though heating at atmospheric pressure did not display this, presumably as some gas molecules remained in the channels (Figure 5). Indeed, as shown in Figure 6, synchrotron XRD of

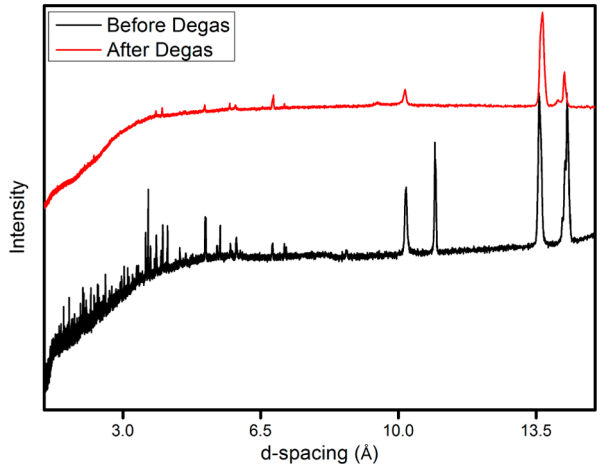

Figure 6. X-ray diffraction before and after solvent evacuation, showing that a degree of structural distortion is responsible for surface area discrepancies.

dx.doi.org/10.1021/cm301726k | *Chem. Mater.* 2012, 24, 4647–4652

Ni-PTC following desolvation *in vacuo* reveals that far fewer diffraction peaks are observed. Together these results indicate that the structurally flexible **Ni-PTC** is prone to crystal distortion upon evacuation, similar to that recently reported by Ma et al.[50]

Ni-PTC exhibits similar strong adsorption characteristics in the adsorption of gases. When exposed to H_2 and CO_2, The framework was found to adsorb in moderate quantities, capturing 0.47 and 8.01 wt % respectively. However, the interaction of the framework with these target analytes was particularly strong. Enthalpies of adsorption were found to be as high as 52.5 kJ mol^{-1} for CO_2 adsorption. Strong binding enthalpies have important implications for the operations under which such materials may be employed. The temperature at which carbon dioxide can be captured from flue gas increases with bonding enthalpy.[51] Values recorded in this instance rank among the highest for CO_2 adsorption in MOFs,[52] and are similar to other materials with exposed Ni^{2+} sites.[53] **Ni-PTC** therefore is a candidate material for the capture of carbon dioxide at elevated temperatures or when present in low concentrations. IAST adsorption selectivity calculations (Figure 7, bottom left) reveal a CO_2/N_2 selectivity of almost 300 at 1 bar and 273 K. This is one of the highest reported performances under these conditions[52] and further underlines the selective nature of the adsorption and its applicability. The adsorption is similarly strong for hydrogen and is also similar to values reported for frameworks with exposed Ni^{2+} sites,[5] which is important in the development of room temperature hydrogen storage. The ideal value for room temperature adsorption in this case is in the range of 15−25 kJ mol^{-1}.[54−56] Similar experiments with Mg-PTC revealed a collapse in the pore architecture on desolvation.

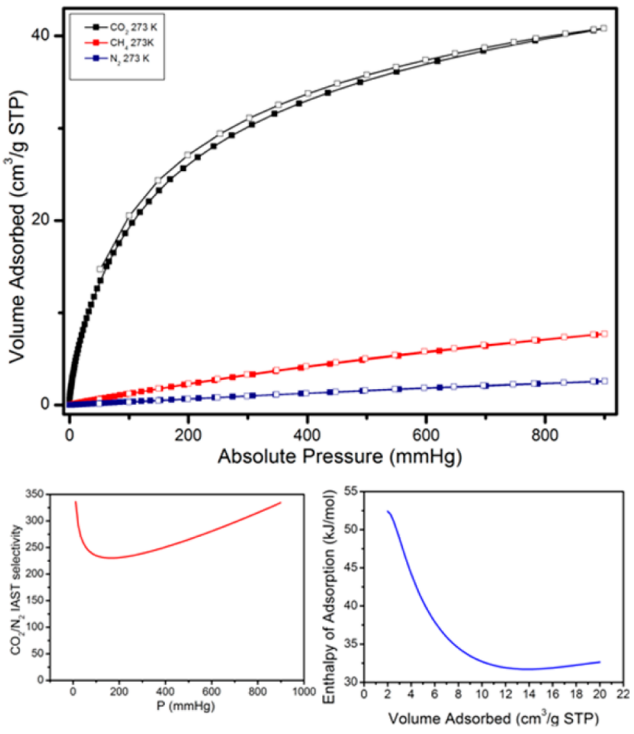

Figure 7. Adsorption selectivity favorable to CO_2 capture is found in **Ni-PTC** (top), which can be attributed to the strong enthalpy of adsorption (bottom, right). IAST adsorption selectivity shows exceptional preference for carbon dioxide over nitrogen (bottom, left).

CONCLUSIONS

A new, moisture resistant series of MOFs have been found to exhibit molecular sieving with size selectivity between subtrates with just 1.6 Å difference in hydrodynamic radii. The utility of this molecular sieving was demonstrated with the capture of the hazardous herbicide, Paraquat. This highly porous series of materials was synthesized in water at room temperature and possessed the same phase for Mg, Ni, Co, and Mn analogues. Consisting of planar M_3O SBUs highly connected to the perylene tetracarboxylic acid ligand (PTC), predicted BET surface areas are above 2000 m^2 g^{-1}. Notably, single crystal quality material can be prepared in water at room temperature, on multigram scales. Structural flexibility in the material results in strong binding interaction, which was further demonstrated in gas adsorption experiments, where CO_2 and H_2 binding enthalpies in excess of 52.5 and 10.75 kJmol^{-1} were observed respectively. The flexibility delivered lower BET surface areas in experiment, being 223 m^2 g^{-1} for desolvated **Ni-PTC**. Further exploitation of the remarkable properties reported herein is ongoing.

ASSOCIATED CONTENT

Supporting Information

Additional information as noted in text and cif files. This material is available free of charge via the Internet at http://pubs.acs.org.

AUTHOR INFORMATION

Corresponding Author

*Fax: 61 3 9545 2837. E-mail: Matthew.hill@csiro.au.

Author Contributions

The manuscript was written through contributions of all authors. All authors have given approval to the final version of the manuscript.

Funding

The authors wish to thank the CSIRO Advanced Materials Transformational Capability Platform for funding

Notes

The authors declare no competing financial interest.

ACKNOWLEDGMENTS

Parts of this work were carried out at the powder diffraction and microcrystallography beamlines at the Australian Synchrotron, Victoria, Australia. D.R.T. acknowledges AINSE for a research fellowship.

REFERENCES

(1) Batten, S. R.; Neville, S. M.; Turner, D. R. *Coordination Polymers: Design, Analysis and Application*; Royal Society of Chemistry: Thomas Graham House, Science Park, Milton Road, Cambridge CB4 0WF, UK, 2008.

(2) Yuan, D.; Lu, W.; Zhao, D.; Zhou, H.-C. *Adv. Mater.* **2011**, *23* (32), 3723−3725.

(3) Sumida, K.; Brown, C. M.; Herm, Z. R.; Chavan, S.; Bordiga, S.; Long, J. R. *Chem. Commun.* **2011**, *47* (4), 1157−1159.

(4) Bae, Y.-S.; Snurr, R. Q. *Microporous Mesoporous Mater.* **2010**, *132* (1−2), 300−303.

(5) Murray, L. J.; Dinca, M.; Long, J. R. *Chem. Soc. Rev.* **2009**, *38* (5), 1294−1314.

(6) Vitillo, J. G.; Regli, L.; Chavan, S.; Ricchiardi, G.; Spoto, G.; Dietzel, P. D. C.; Bordiga, S.; Zecchina, A. *J. Am. Chem. Soc.* **2008**, *130* (26), 8386−8396.

(7) Venna, S. R.; Carreon, M. A. *J. Am. Chem. Soc.* **2010**, *132*, 76−78.

(8) Bohrman, J. A.; Carreon, M. A. *Chem. Commun.* **2012**, *48* (42), 5130−5132.
(9) Liu, Y.; Zeng, G.; Pan, Y.; Lai, Z. *J. Membr. Sci.* **2011**, *379* (1−2), 46−51.
(10) Huang, Q.; Cai, J.; Wu, H.; He, Y.; Chen, B.; Qian, G. *J. Mater. Chem.* **2012**, *22* (20), 10352−10355.
(11) Thornton, A. W.; Nairn, K. M.; Hill, J. M.; Hill, A. J.; Hill, M. R. *J. Am. Chem. Soc.* **2009**, *131* (30), 10662−10669.
(12) Sumida, K.; Hill, M. R.; Horike, S.; Dailly, A.; Long, J. R. *J. Am. Chem. Soc.* **2009**, *131* (42), 15120−15121.
(13) Sun, C. Y.; Qin, C.; Wang, C. G.; Su, Z. M.; Wang, S.; Wang, X. L.; Yang, G. S.; Shao, K. Z.; Lan, Y. Q.; Wang, E. B. *Adv. Mater.* **2011**, *23* (47), 5629−5631.
(14) Pandolfo, A. G.; Hollenkamp, A. F. *J. Power Sources* **2006**, *157* (1), 11−27.
(15) Zhao, J. C.; Lai, C. Y.; Dai, Y.; Xie, J. Y. *J. Cent. South Univ. Technol. (Engl. Ed.)* **2005**, *12* (6), 647−652.
(16) Fan, J.; Yu, C.; Wang, L.; Tu, B.; Zhao, D.; Sakamoto, Y.; Terasaki, O. *J. Am. Chem. Soc.* **2001**, *123* (48), 12113−12114.
(17) Lukens, W. W.; Schmidt-Winkel, P.; Zhao, D. Y.; Feng, J. L.; Stucky, G. D. *Langmuir* **1999**, *15* (16), 5403−5409.
(18) Hill, M. R.; Pas, S. J.; Mudie, S. T.; Kennedy, D. F.; Hill, A. J. *J. Mater. Chem.* **2009**, *19* (15), 2215−2225.
(19) Boskovic, S.; Hill, A. J.; Turney, T. W.; Gee, M. L.; Stevens, G. W.; O'Connor, A. J. *Prog. Solid State Chem.* **2006**, *34* (2−4), 67−75.
(20) Hill, M. R.; Wilson, G. J.; Bourgeois, L.; Pandolfo, A. G. *Energy Environ. Sci.* **2011**, *4* (3), 965−972.
(21) Hill, M. R.; Booth, J.; Bourgeois, L.; Whitfield, H. J. *Dalton Trans.* **2010**, *39* (22), 5306−5309.
(22) Rumplecker, A.; Kleitz, F.; Salabas, E. L.; Schuth, F. *Chem. Mater.* **2007**, *19* (3), 485−496.
(23) Jiang, H.-L.; Tatsu, Y.; Lu, Z.-H.; Xu, Q. *J. Am. Chem. Soc.* **2010**, *132* (16), 5586−5587.
(24) Jiang, H.-L.; Xu, Q. *Chem. Commun.* **2011**, *47* (12), 3351−3370.
(25) Lan, Y.-Q.; Jiang, H.-L.; Li, S.-L.; Xu, Q. *Adv. Mater.* **2011**, *23* (43), 5015−5020.
(26) Wong-Foy, A. G.; Matzger, A. J.; Yaghi, O. M. *J. Am. Chem. Soc.* **2006**, *128* (11), 3494−3495.
(27) D'Alessandro, D. M.; McDonald, T. *Pure Appl. Chem.* **2010**, *83* (1), 57−66.
(28) D'Alessandro, D. M.; Smit, B.; Long, J. R. *Angew. Chem., Int. Ed.* **2010**, *49* (35), 6058−6082.
(29) Li, J. R.; Kuppler, R. J.; Zhou, H. C. *Chem. Soc. Rev.* **2009**, *38* (5), 1477−1504.
(30) Eddaoudi, M.; Kim, J.; Rosi, N.; Vodak, D.; Wachter, J.; O'Keeffe, M.; Yaghi, O. M. *Science* **2002**, *295* (5554), 469−472.
(31) Dinca, M.; Long, J. R. *Angew Chem., Int. Ed.* **2008**, *47* (36), 6766−6779.
(32) Rowsell, J. L. C.; Yaghi, O. M. *Angew. Chem., Int. Ed.* **2005**, *44* (30), 4670−4679.
(33) Kaye, S. S.; Dailly, A.; Yaghi, O. M.; Long, J. R. *J. Am. Chem. Soc.* **2007**, *129* (46), 14176−14167.
(34) Bajpe, S. R.; Kirschhock, C. E. A.; Aerts, A.; Breynaert, E.; Absillis, G.; Parac-Vogt, T. N.; Giebeler, L.; Martens, J. A. *Chem.—Eur. J.* **2009**, *16* (13), 3926−3932.
(35) Ramanan, A.; Whittingham, M. S. *Cryst. Growth Des.* **2006**, *6* (11), 2419−2421.
(36) Colombo, V.; Galli, S.; Choi, H. J.; Han, G. D.; Maspero, A.; Palmisano, G.; Masciocchi, N.; Long, J. R. *Chem. Sci.* **2011**, *2* (7), 1311−1319.
(37) Salles, F.; Maurin, G.; Serre, C.; Llewellyn, P. L.; Knoefel, C.; Choi, H. J.; Filinchuk, Y.; Oliviero, L.; Vimont, A.; Long, J. R.; Ferey, G. *J. Am. Chem. Soc.* **2010**, *132* (39), 13782−13788.
(38) Choi, H. J.; Dinca, M.; Dailly, A.; Long, J. R. *Energy Environ. Sci.* **2010**, *3* (1), 117−123.
(39) Liu, J.; Wang, Y.; Benin, A. I.; Jakubczak, P.; Willis, R. R.; LeVan, M. D. *Langmuir* **2010**, *26* (17), 14301−14307.
(40) Fu, Y.; Sun, D.; Chen, Y.; Huang, R.; Ding, Z.; Fu, X.; Li, Z. *Angew Chem., Int. Ed.* **2012**, *51* (14), 3364−3367.
(41) Luo, F.; Batten, S. R. *Dalton Trans.* **2010**, *39*, 4485−4488.
(42) Spietschka, E.; Urban, M. Perylene-3,4,9,10-tetra:carboxylic di:anhydride prodn.|by hydrolysis of the di:carboximide. EP205980-A1; DE3520807-A; JP61286385-A; US4650879-A; EP205980-B; DE3661533-G, 1986.
(43) McPhillips, T. M.; McPhillips, S. E.; Chiu, H. J.; Cohen, A. E.; Deacon, A. M.; Ellis, P. J.; Garman, E.; Gonzalez, A.; Sauter, N. K.; Phizackerley, R. P.; Soltis, S. M.; Kuhn, P. *J. Synchrotron Radiat.* **2002**, *9*, 401.
(44) Kabsch, W. *J. Appl. Crystallogr.* **1993**, *26*, 795.
(45) Wall, A. J.; Heaney, P. J.; Mathur, R.; Post, J. E.; Hanson, J. C.; Eng, P. J. *J. Appl. Crystallogr.* **2011**, *44* (2), 429−432.
(46) *Materials Studio, 5.0*; Accelrys Inc.: San Diego, CA, USA, 2009.
(47) Caskey, S. R.; Wong-Foy, A. G.; Matzger, A. J. *J. Am. Chem. Soc.* **2008**, *130*, 10870.
(48) Dietzel, P. D. C.; Blom, R.; Fjellvag, H. *Eur. J. Inorg. Chem.* **2008**, 3624.
(49) Tanner, C. M.; Kamel, F.; Ross, G. W.; Hoppin, J. A.; Goldman, S. M.; Korell, M.; Marras, C.; Bhudhikanok, G. S.; Kasten, M.; Chade, A. R.; Comyns, K.; Richards, M. B.; Meng, C.; Priestley, B.; Fernandez, H. H.; Cambi, F.; Umbach, D. M.; Blair, A.; Sandler, D. P.; Langston, J. W. *Environ. Health Perspect.* **2011**, *119* (6), 866−872.
(50) Ma, L. Q.; Falkowski, J. M.; Abney, C.; Lin, W. B. *Nat. Chem.* **2010**, *2* (10), 838−846.
(51) Demessence, A.; D'Alessandro, D. M.; Foo, M. L.; Long, J. R. *J. Am. Chem. Soc.* **2009**, *131* (25), 8784−8786.
(52) Sumida, K.; Rogow, D. L.; Mason, J. A.; McDonald, T. M.; Bloch, E. D.; Herm, Z. R.; Bae, T.-H.; Long, J. R. *Chem. Rev.* **2012**, *112* (2), 724−781.
(53) Dietzel, P. D. C.; Johnsen, R. E.; Fjellvag, H.; Bordiga, S.; Groppo, E.; Chavan, S.; Blom, R. *Chem. Commun.* **2008**, 5125.
(54) Bhatia, S. K.; Myers, A. L. *Langmuir* **2006**, *22* (4), 1688−1700.
(55) Garrone, E.; Bonelli, B.; Otero-Arean, C. *Chem. Phys. Lett.* **2008**, *456* (1), 68−70.
(56) Otero-Arean, C.; Chavan, S.; Cabello, C. P.; Garrone, E.; Palomino, G. T. *ChemPhysChem* **2010**, *11*, 3237.